Quaternary Structure Sensitive Tyrosine Interactions in Hemoglobin: A UV Resonance Raman Study of the Double Mutant rHb (*β*99Asp→Asn, α42Tyr→Asp)†

Shoucai Huang,‡ Eric S. Peterson,‡ Chien Ho,§ and Joel M. Friedman*,‡

Department of Physiology and Biophysics, Albert Einstein College of Medicine, Bronx, New York, 10461, and Department of Biological Sciences, Carnegie Mellon University, Pittsburgh, Pennsylvania 15213-2583

Received January 2, 1997⊗

ABSTRACT: Two interactions involving tyrosines have been implicated in the communication pathway that links ligand binding to quaternary state changes in hemoglobin. Tyr $\alpha_1$42 stabilizes the $\alpha_1\beta_2$ T state interface through the formation of a hydrogen bond to Asp $\beta_2$99. The side chains of the penultimate Tyr residues (α140 and *β*145) occupy the pockets made by helicies F and H in the deoxy form with the phenolic hydroxyl hydrogen bonded to the carbonyl group of Val FG5. Early crystallographic studies indicated that in the R form the penultimate Tyr is expelled out of the pocket, thus eliminating the hydrogen bond. This hydrogen bond has been considered to play an important role in maintaining the low-oxygen-affinity state (T state) in deoxy HbA, but a later higher resolution crystallographic study (Shannon, 1983) failed to reveal such movement of this Tyr during the R → T transition. Nevertheless, conversion of this Tyr to Phe increases oxygen affinity considerably, suggesting that hydrogen bonding is involved in oxygen affinity modulation. Earlier ultraviolet resonance Raman results reported by Spiro and co-workers [Rodgers et al. (1992) *J. Am. Chem. Soc. 114*, 3697−3709] were used to conclude that the significant quaternary structure dependent changes observed in tyrosine Raman bands are due to the formation of the T state hydrogen bond with Tyr α42 acting as a proton acceptor rather than being the anticipated proton donor, as would be expected if Asp *β*99 were ionized. This surprising result rests on the assumption that changes in the environment of Tyr α42 are the overwhelming contributor to the R − T UV Raman difference spectrum. In this study, a cooperative double mutant lacking Tyr α42, [rHb (Asp *β*99 → Asn, Tyr α42 → Asp)], is used to determine the relative contributions of Tyr α42 and the penultimate tyrosines to the R − T UV resonance Raman difference spectrum. The results both directly support the claim that Tyr α42 is the proton acceptor in the T state and expose the potential role of the penultimate tyrosines in coupling the quaternary state to the ligand reactivity.

Hemoglobin is a tetrameric protein molecule composed of two pairs of similar subunits. Each subunit contains a heme group, where oxygen, or other ligands, binds reversibly. The heme group is linked to the globin by a covalent bond from the heme iron to a histidine residue, known as the proximal histidine. The oxygen affinity of the hemoglobin molecule rises with increasing oxygen occupancy. The search for the structural explanation of this cooperativity, or heme−heme interaction, has made hemoglobin one of the most intensely studied proteins.

The three-dimensional structures of deoxy (Fermi et al., 1984) and liganded hemoglobin (Shaanan, 1983) have been determined by X-ray analysis [for a review see Perutz et al. (1987) and Perutz (1989)]. It had been shown that the quaternary structure of deoxy hemoglobin differs from that of liganded hemoglobin and that cooperativity is associated with the quaternary structure change that takes place upon ligation. Until recently it had been assumed that there were only two quaternary states to consider in the analysis of cooperativity: the low-affinity T structure associated with the deoxy species and the high-affinity R structure associated with the fully liganded species. X-ray crystallographic studies on COHb Ypsilanti (D*β*99Y) (Smith et al., 1991), low salt crystals of COHbA (Silva et al., 1992), and CNHbA (Smith & Simmons, 1994) reveal the existence of a third quaternary structure designated Y or R2. Thermodynamic studies (Bucci et al., 1993) suggest that R2 may lie on the pathway between T and R (as the triply liganded species), whereas modeling studies (Srinivasan & Rose, 1994) suggest that R2 is in fact the solution phase liganded species and that the crystallographic R structure is an intermediate between T and R2. A major difficulty in addressing this issue is the absence of any clear spectroscopic marker to differentiate between R and R2 in solution.

Regardless of whether the R2 or R structure is a dominant solution phase equilibrium structure, it is clear that a complete detailed understanding of hemoglobin cooperativity at a molecular level remains elusive in spite of impressive advances obtained through extensive thermodynamic analysis (Ackers et al., 1992), theoretical treatments (Gellin et al., 1983) and structural investigations using X-ray diffraction, UV−visible, NMR, and other techniques over the past decades (Antonini & Brunori, 1971; Baldwin & Chothea, 1979; Fung et al., 1976, 1977; Perutz, 1987; Dickerson & Geis, 1983; Rousseau & Friedman, 1988; Friedman, 1994; Fung & Ho, 1975, Viggiano & Ho, 1979; Ho, 1992; Shen

† This work funded by grants from the W. M. Keck Foundation (J.M.F.) and the NIH RO1-GM44343 (J.M.F.), PO1HL51084 (J.M.F.), HL-58249 (C.H.), and HL-24525 (C.H.).

* Corresponding author. Tel: (718) 430-3591. Fax: (718) 430-8819. E-mail: jfriedma@aecom.yu.edu).

‡ Albert Einstein College of Medicine.

§ Carnegie Mellon University.

⊗ Abstract published in *Advance ACS Abstracts,* April 15, 1997.

S0006-2960(97)00018-4 CCC: $14.00

et al., 1993; Kim et al., 1994, 1995, 1996; Liddington, 1994; Jayaraman et al., 1993, 1995). A significant hurdle has been the failure to identify the important interactions which link tertiary and quaternary alternations to heme structural changes at the site of oxygen binding. Some progress has been made by obtaining structures of a series of deoxy and liganded structures locked into a given quaternary state [see, for example, Arnone et al. (1986) and Abraham et al. (1992)].

One difficulty in the pursuit of molecular level investigations of the structural basis for reactivity is that changes in bond strengths that may have a profound influence on reactivity or stability can arise from changes in distances that are beyond the routine resolution of X-ray crystallography. Such changes can often be most directly probed through vibrational spectroscopy, which provides a direct measure of the vibrational frequency of specific modes in solution phase protein samples.

Resonance Raman spectroscopy has provided a considerable amount of detail regarding the influence of tertiary and quaternary structure upon specific heme related vibrational degrees of freedom. In particular, the iron-proximal histidine stretching frequency (Kitagawa, 1988, 1992; Rousseau & Friedman, 1988; Friedman, 1985, 1994) has been shown both to couple directly to the tertiary and quaternary structure and to be a direct reflection of proximal strain—a major determinant of ligand-binding reactivity.

More recently, advances in ultraviolet resonance Raman spectroscopy (Asher 1993; Kitagawa, 1992; Austin et al., 1993; Jayaraman et al., 1995) have allowed for comparably detailed studies of vibrational modes within the globin that reflect key interactions involving aromatic residues. Spiro and co-workers (Rodgers et al., 1992) assigned one particular deoxy versus oxy change in a tyrosine specific Raman band as being due to the functionally important change (LiCata et al., 1993; Hashimoto et al., 1993) in the hydrogen bond between Tyr α42 and Asp β99. There are structural (X-ray, Raman, NMR) and functional studies (Fung & Ho, 1975; Reed et al., 1977; Jones et al., 1967; Rucknagel et al., 1967; Kim et al., 1994, 1996; Ishimori et al., 1992; Imai et al., 1991) that have highlighted the changes in this particular hydrogen bond as being a key determinant of quaternary stability and oxygen affinity. This hydrogen bond contributes significantly to the stability of the T-state structure, but is broken in the R structure. The UV Raman data clearly support these previous findings, but indicate that the standard assumption (Baldwin & Chothia, 1979) that the tyrosyl proton is hydrogen bonded to an ionized aspartic acid carboxylate in the T state is incorrect (Rodgers et al., 1992). The Raman results indicate that the tyrosine and not the carboxyl of β99 is the proton acceptor with the obvious consequence that the carboxyl group is not ionized.

The analysis of the tyrosine Raman data is based on the assumption that the changes observed in the Raman bands in question are overwhelmingly due to the loss of hydrogen bonding between Tyr α42 and Asp β99 upon switching from T to R. There is, however, another anticipated change that could contribute to the observed changes, and this possibility complicates the analysis. The side chains of the penultimate tyrosine residues, α140 (HC2) and β145 (HC2), are believed to change their interaction with the FG corner as a function of quaternary state on the basis of X-ray crystallographic studies. This interaction is of potential importance both in the control of protein conformation and reactivity as well as for the spectroscopic reasons discussed above. Part of the UV resonance Raman difference spectrum could originate from the changes associated with this residue.

In all of the vertebrate hemoglobins and myoglobins whose sequence structures have been elucidated, the penultimate position, HC2, is invariably occupied by tyrosine. The natural Hb mutants which have the mutation at this position, such as Hb Osler (Tyr β145 → Asp) (Charache et al., 1975; Viggiano et al., 1978), Hb Bethesda (Tyr β145 → His) (Hayashi & Stamatoyannopoulos, 1972), Hb Rainier (Tyr β145 → Cys) (Hayashi & Stamatoyannopoulos, 1972), and Hb McKees Rocks (Tyr β145 → terminated) (Viggiano et al., 1978), fail to retain the T state conformation in the deoxygenated form, resulting in extremely high oxygen affinities and absence of cooperativity. Des-(His β146, Tyr β145) Hb, in which the terminal histidine and penultimate Tyr were removed by carboxypeptidase, also shows a marked increase in oxygen affinity and greatly diminished cooperativity (Bonaventura et al., 1972).

X-ray crystallographic studies of deoxy HbA reveal that the penultimate tyrosine of the α and β subunits are hydrogen bonded to the carbonyls of Val α94 and Val β98, respectively, at the FG corner (position FG5) of the same subunit. Initial studies (Baldwin & Chothia, 1979) suggested that this hydrogen bond is lost in going from T to R and that the tyrosine is expelled from the pocket formed by the H and F helices (which we will refer to as the H−F pocket). Subsequent studies (Shaanan, 1983) indicate that the tyrosine is not expelled from the H−F pocket and that there is only an increase in the degree of disorder of the tyrosyl group in going to the R quaternary state. The hydrogen bond is likely to be important functionally in that it may serve to anchor the F helix in an appropriate position to increase proximal strain at the heme-proximal histidine interface and thus facilitate the decrease in ligand affinity associated with the T state. A weakening of this hydrogen bond could allow the F helix to shift more readily to its R state position (toward the FG corner) upon ligand binding. In addition, the hydrogen bond between the tyrosine and the valine may stabilize the T state interactions of the C-terminus within the $\alpha_1\beta_2$ interface.

Detecting conformational changes in proteins at an atomic level lies at the very heart of current biophysical research. With the advance of protein engineering, it is now possible to introduce mutations at desired sites of a given protein. This technique provides a way of pinpointing the functional role of a particular residue in hemoglobin by replacing it with a different residue. In this work, we use UV and visible resonance Raman spectroscopy to examine the deoxy versus liganded differences in the double mutant recombinant hemoglobin, rHb (Asp β99 → Asn, Tyr α42 → Asp), which is missing Tyr α42 and yet retains cooperativity at pH 7.2 (Kim et al., 1994). This rHb offers us an opportunity to examine the behavior of the tyrosine Raman spectral bands during the ligand binding induced conformational transition without interference from Tyr α42. By using the double mutant to eliminate the signal from Tyr α42, it is anticipated both that the behavior associated with the penultimate tyrosines can be exposed and that the assignment made by the Spiro group (Rodgers et al., 1992) regarding the nature of the Tyr α42 and Asp β99 hydrogen bond can be unambiguously tested.

EXPERIMENTAL PROCEDURES

Preparation of Human Adult Hemoglobin

Hemolysates from AC and CC individuals' washed red blood cells were made by freeze−thawing with the cellular debris separated by centrifugation. The hemoglobins were separated and purified on a CM-52 column as previously described (Schroeder et al., 1980). The isolation was verified by isoelectric focusing.

Preparation of Hemoglobin Double Mutant

Purification of rHb (β:D99N, α:Y42D). Frozen *Escherichia coli* cell pellets for rHb (β:D99N, α:Y42D) derived from the expression plasmid pHE222 were stirred gently in lysis buffer (40 mM Tris base) at 4 °C until they were completely thawed. Lysozyme (ICN) and DNase (Calbiochem) were then added, and the lysate was sonicated. The lysate was then centrifuged to pellet cell membrane, etc., and the supernatant adjusted to pH 8.3 with 1 M Tris base and then put through a Millipore Minitan acrylic ultrafiltration system to concentrate and, at the same time, equilibrate the protein for the first column. Two columns were used in purification of the protein: (i) The first column, a Q-Sepharose Fast Flow anion-exchanger K(Pharmacia), was used to bind the Hb. The column was then washed with 20 mM Tris·HCl/0.1 mM TETA at pH 8.3, and the eluent was monitored at 260 nm until all of the nucleic acid is eluted. The bound Hb was then eluted with 20 mM Tris·HCl/0.1 mM TETA at pH 7.2. (ii) The second column, a Mono S cation exchanger (Pharmacia HR 16/10), was used to further purify the Hb. The Hb is eluted by using a gradient of 10 mM sodium phosphate/0.1 mM EDTA at pH 6.8 to 20 mM sodium phosphate/0.1 mM EDTA at pH 8.2. One major fraction was eluted from the Mono S column, and this was used for all our studies. For details, refer to Kim et al. (1994).

Mass Spectromeric Studies and N-Terminal Sequencing. Mass spectrometric and N-terminal sequencing analysis showed that rHb (β:D99N, α:Y42D) has the correct molecular weight for the Tyr → Asp replacement on the α chain and the Asp → Asn replacement on the β chain and that the N-terminal methionine residues of both the α and β chains have been effectively cleaved by the co-expressed methionine aminopeptidase. For details, see Kim et al. (1994).

UV Raman Spectroscopy

The UV resonance Raman spectrometer was composed of a laser source, a 1.5*M* single spectrograph equipped with a 3600 groove/mm holographic grating, and a liquid N_2 cooled CCD detector. The CCD detector (Princeton Instrument, NJ) had a UV metachrome coating on its chip. The intracavity frequency-doubled ring dye laser (Coherent 899) utilized stilbene 420 and was pumped by the multi-UV line output of an Argon ion laser (Coherent Innova 400). In the present work, we have modified the ring dye laser. To maximize the UV output with acceptable bandwidth, we used the thin etalon only instead of two etalons (thick and thin). This laser system generated CW UV output from 218 to 240 nm. The maximum output of this system at 226 nm was 6 mW. In this experiment, the average UV power used was ∼1 mW at 229 nm, which has proven to be sufficient for acquiring high-quality Raman spectra. The sample was held in a quartz tube for data collection. During the period of data acquisition, the tube was maintained at 10 °C and spun in a helical fashion at 5 Hz, so that the incoming laser beam would not always impinge upon the same spot. The scattered photons were collected with a triplet lens (Fused suprasil, CVI Laser Corporation) and focused onto the entrance slit (270 μm) of the 1.6M spectrograph (Sopra Inc., France). The spectra were calibrated with the use of the Raman spectra of cyclohexane and 1,4-dioxane. For the UV Raman data presented here, spectral acquisitions were carried out as a series of 5-min accumulations, and each final spectrum was the sum of three to five of these 5-min spectra. Before the spectra were summed, cosmic rays were removed from each spectrum using SpectraCalc software (Galactic Industries Corporation). Also each spectrum was subtracted from the first one taken from a given sample. If difference features were observed, the spectrum was discarded. Finally, the spectral intensities were normalized prior to taking a difference spectrum by equalizing the heights of the peak at 934 cm^{-1} which is due to the presence of added sodium perchlorate as an internal intensity standard.

The UV Raman spectra of HbA and rHb were obtained for samples (∼0.8 mM in heme) at pH 7.30 (50 mM bis-Tris) and 7.0 (50 mM phosphate), respectively. Under these conditions both proteins bind oxygen cooperatively, although the mutant does have a reduced Hill coefficient relative to HbA (Kim et al., 1994). The lower pH and phosphate buffer for rHb are used to increase the cooperativity in this mutant in order to maximize the population of the T state in the deoxy form.

Visible Resonance Raman Spectroscopy

CO derivatives were prepared from oxy stock solutions by passing CO gas over the surface of a 100 μL aliquot in a sealed vial. Deoxy derivatives were prepared by passing N_2 over the sample and then adding 5 equiv with respect to heme concentration of sodium dithionite. All samples were approximately 2 mM in heme and were in 50 mM potassium phosphate buffer, pH 7.0. The samples were then loaded in a nitrogen atmosphere into quartz sample cells with a 200 μm path length. (Helma P/N 124-QS, Jamaica, NY). The front window of the cell was replaced with a sapphire window, which yielded a flatter base line in the low-frequency region of the Raman spectrum. The sample cell was mounted in a custom brass holder, which was cooled to approximately 10 °C and rotated fast enough such that a new sample volume was interrogated with each laser shot. Photoproduct buildup and artifacts from sample spinning were found to be negligible by varying the spinning rate and by taking visible absorption spectra before and after each experiment.

Visible time-resolved resonance Raman spectra were obtained using an 8 ns 435.8 nm pulse both to photodissociate the ligand and to Raman scatter off the sample. A Nd:YAG laser was used (Continuum NY81C-20, Santa Clara, CA), which produced 450 mJ pulses at 20 Hz in the second harmonic output at 532 nm. 4 W of the 532 nm beam was focused into a homemade 90 cm long cell filled with 120 psi of hydrogen to Raman shift the laser to 435.8 nm. Neutral density filters were used to reduce the energy of the 435.8 nm pulses to 150 μJ and these were focused with a 150 mm plano-convex lens on the sample at an incident angle of 45°. The Raman scattered light was collected at

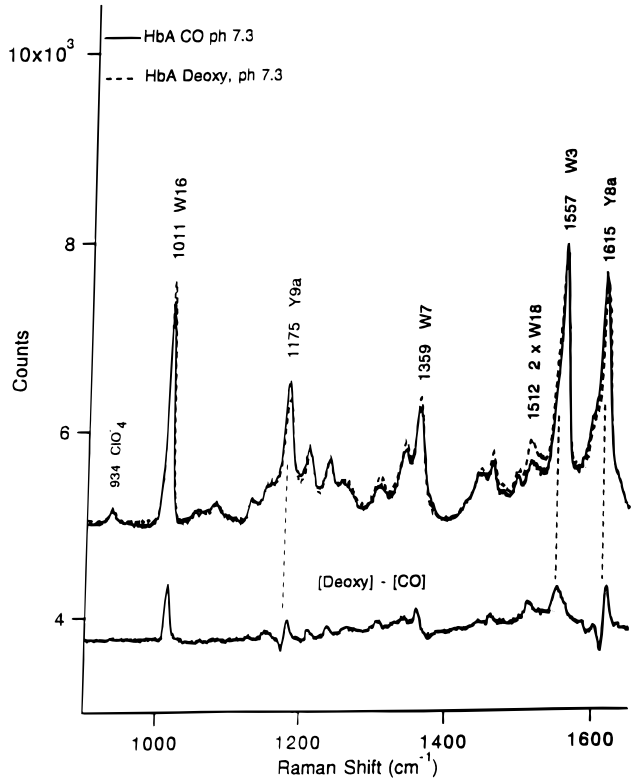

FIGURE 1: Comparison of the CW (continuous wave) UV resonance Raman spectra of the deoxy and carbonmonoxy derivatives of human adult hemoglobin generated by 1.1 mW of 229 nm excitation. The bottom of the figure shows the difference spectrum which is normalized using the 934 cm^{-1} perchlorate Raman band as an internal intensity reference.

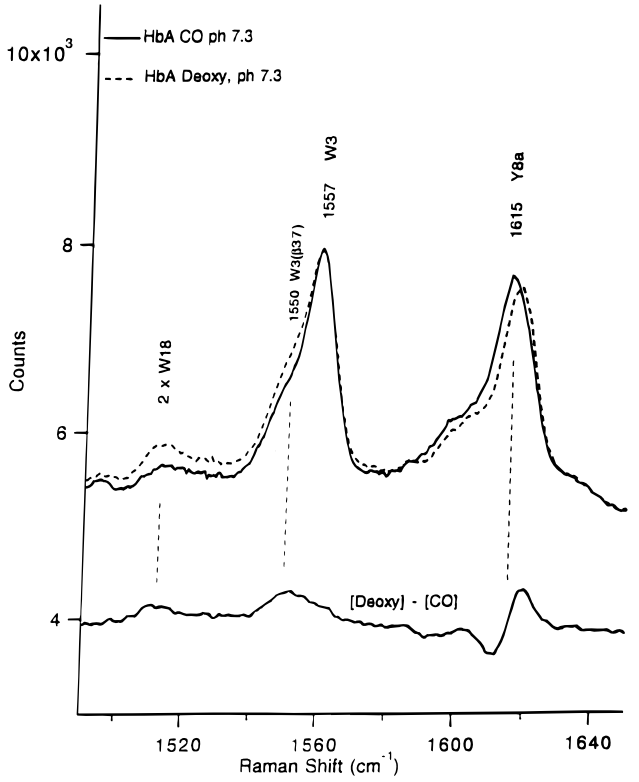

FIGURE 2: Expansion of the 1480−1670 cm^{-1} region of Figure 1.

normal incidence to the sample (135° to the laser) with a 50 mm Nikon F/1.4 camera lens and focused with an *f*-matching lens onto the 100 μm × 5 mm slit of a 0.64 m single monochromator utilizing an 1800 grooves/mm grating (ISA HR640, Metuchen, NJ). The Rayleigh line was reduced in intensity with a holographic notch filter (Kaiser P/N HNF-1171 centered at 442 nm, Ann Arbor, MI), and a depolarizer (CVI P/N DPL-10, Putnam, CT) was used to scramble the polarization of the collected light and thus eliminate intensity artifacts created by polarization dependent grating reflectivity. The detector was an intensified diode array run in the CW mode (Princeton Instruments P/N IRY-1024S/B, Trenton, NJ). The total accumulation time per spectrum was typically 30 min. The spectral bandwidth of the monochromator was approximately 5 cm^{-1}, and the discretization on the detector face was approximately 0.9 cm^{-1} per pixel. Raman spectra were calibrated using solvent spectra with previously determined peak assignments. A least squares fit was used to map pixel number into relative wavenumbers (Raman shift). The Raman spectra were baselined using a polynomial fitting routine in LabCalc (Galactic Industries, Salem, NH) and are presented without smoothing.

RESULTS AND DISCUSSION

HbA: Deoxy versus CO Difference Spectrum

Figure 1 shows the high-frequency regions of the 229 nm excited UV resonance Raman spectra of the deoxy and CO derivatives of HbA. Figure 2 shows the region above 1500 cm^{-1} in greater detail. The Raman band labeled Y8a (∼1615 cm^{-1} in Figures 1 and 2) and its weaker shoulder due to Y8b (∼1600 cm^{-1}, not labeled in Figures 1 and 2) both arise from tyrosine side chains. They show strong difference signals. These bands arise from six symmetry-related pairs of Tyr residues, yet no apparent spectral inhomogeneity is observed. Upon switching from the CO to the deoxy derivative of HbA, these bands clearly shift to higher frequency and display lower intensity as reported in previous studies (Rodgers et al., 1992). As shown previously (Rodgers et al., 1992), contributions from phenylalanine residues are negligible at this excitation wavelength. Among the six tyrosines, the following tyrosine residues were assumed by Rodgers et al. (1992) to be unaltered during the R → T transition on the basis of analysis of X-ray crystallographic coordinates for carbonmonoxy- and deoxy-Hb: Tyr α24 (B helix), Tyr β130 (H helix), and Tyr α35 ($\alpha_1\beta_1$ interface). The possible contributions come from Tyr α42 and the C-termini tyrosine residues: α140 and β145. Rodgers et al. (1992) discounted the potential contribution from the C-termini tyrosine residues and interpreted the spectral changes in Y8a/Y8b resulting from the hydrogen bond formation between Tyr α42 and Asp β99 during the quaternary transition occurring upon deligation.

Other CO − deoxy differences are also apparent in the HbA spectra. The W3 tryptophan band at ∼1557 cm^{-1}, in Figures 1 and 2, is sensitive to both the dihedral angle of the indole ring and the strength of the hydrogen bonds between the indole and adjacent residues (Austin et al., 1993). The W3 band is composed of two populations (Rodgers et al., 1992). There is a low-frequency shoulder at 1550 cm^{-1} which has been assigned to Trp β37. The main portion of the band centered at 1558 cm^{-1} arises from the combined contribution of the four tryptophans on the A helices: Trp β15 and Trp α14. The difference in the peak position of these two bands arises from differences in the dihedral angle of the indole rings. It can be seen that the major CO −

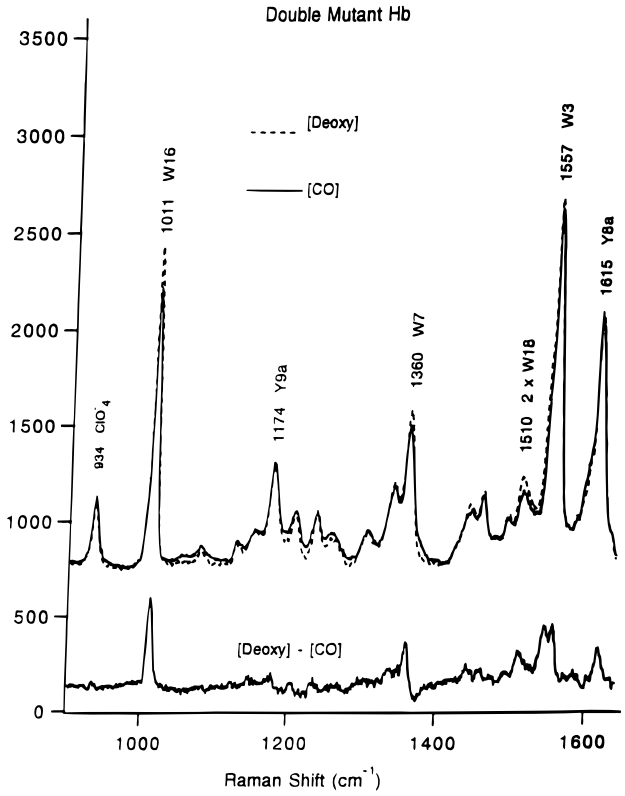

FIGURE 3: 229-nm excited UV resonance Raman spectra of the deoxy (dashed line) and carbonmonoxy (solid line) derivatives of the recombinant hemoglobin. The bottom of the figure shows the difference spectrum which is normalized using the 934 cm^{-1} perchlorate Raman band as an internal intensity reference.

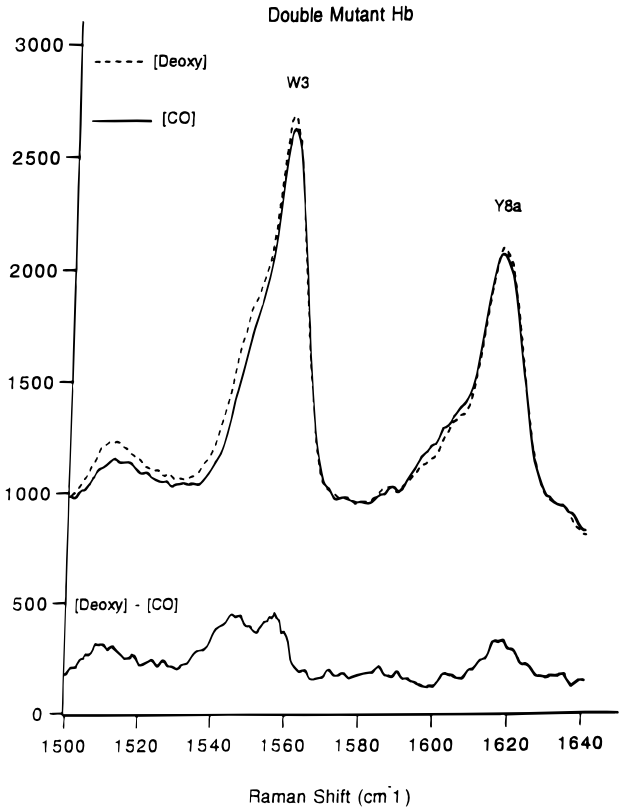

FIGURE 4: Expansion of the 1480−1670 cm^{-1} region of Figure 3.

deoxy difference associated with W3 arises from the β37 shoulder as previously reported (Rodgers et al., 1992). The CO − deoxy difference is predominantly a change in intensity which is ascribed (Nagai et al., 1995) to the loss of the hydrogen bond between Trp β37 and Asp α94 in the flexible joint region of the $\alpha_1\beta_2$ subunit interface upon ligand binding (and change of quaternary state).

The pair of bands at ∼1359 cm^{-1} in Figure 1 is a Fermi doublet associated with tryptophan. The ratio of the higher frequency band to the lower is a reflection of the degree of hydrophobicity of the tryptophan environment (Austin et al., 1993). It can be seen that there is little change in going from deoxy to CO HbA.

The difference peak at ∼1510 cm^{-1} has been identified as an R − T difference marker of uncertain origin (possibly the second harmonic of W18) that can be used to determine the extent of change in the population of a given quaternary state (Jayaraman et al., 1993).

rHb: CO − Deoxy UV Resonance Raman Difference Spectrum

Figure 3 shows the high-frequency regions of the 229 nm excited resonance Raman spectra of the deoxy and CO derivatives of the recombinant Hb at pH 7.0 (50 mM phosphate buffer). Figure 4 shows the spectral region above 1500 cm^{-1}. It can be seen from the figures that the quaternary state difference marker at 1510 cm^{-1} is prominent, indicating that there is a quaternary transition occurring upon deoxygenation as anticipated from functional studies. The Trp β37 component of the W3 band at ∼1550 cm^{-1} also shows the anticipated CO − deoxy difference pattern.

In HbA, the tryptophan α14/β15 component of W3 at 1557 cm^{-1} is not noticeably changed during the CO − deoxy transition, but in rHb, this band does appear to change upon deoxygenation. The deoxy species shows an intensity gain relative to the CO derivative. A comparison with HbA of like derivatives (CO or deoxy) indicates that this difference between the two proteins originates in the CO derivative. A likely source of this difference is the high concentration of phosphate used with the mutant hemoglobin. High concentrations of phosphate do perturb the CO-bound state of HbA as reflected in the visible resonance Raman spectrum (*vide infra*). Preliminary UV resonance Raman measurements (Friedman, unpublished) on COHbA in the presence of IHP revealed changes in the α14/β15 component similar to what is observed in the present study. Since both phosphate and IHP bind to the DPG binding site at the β subunit end of the central cavity, it is plausible that as a result, the A helix of the β subunit is perturbed. A UV resonance Raman study (Hirsch et al., 1995) of HbC (β6 Glu → Lys) showed that a mutation-induced perturbation of the A helix can be reflected in the α14/β15 component of W3.

In contrast to the substantial CO − deoxy changes in the Y8a tyrosine band observed in HbA, the double mutant shows essentially no frequency shift in going from the CO form to the deoxy form, but the intensity of this band does increase. Given the known crystallographic information as to which tyrosines undergo changes upon deoxygenation (Rodgers et al., 1992), we attribute this difference to a change in the environment of the C-termini tyrosine residues in going from the liganded to deoxy state.

The CO − deoxy spectroscopic behavior of the rHb differs from HbA in an additional fashion with regard to the tyrosine bands in the UV resonance Raman spectrum. It can be seen in Figure 3 that in contrast to native HbA, the double mutant

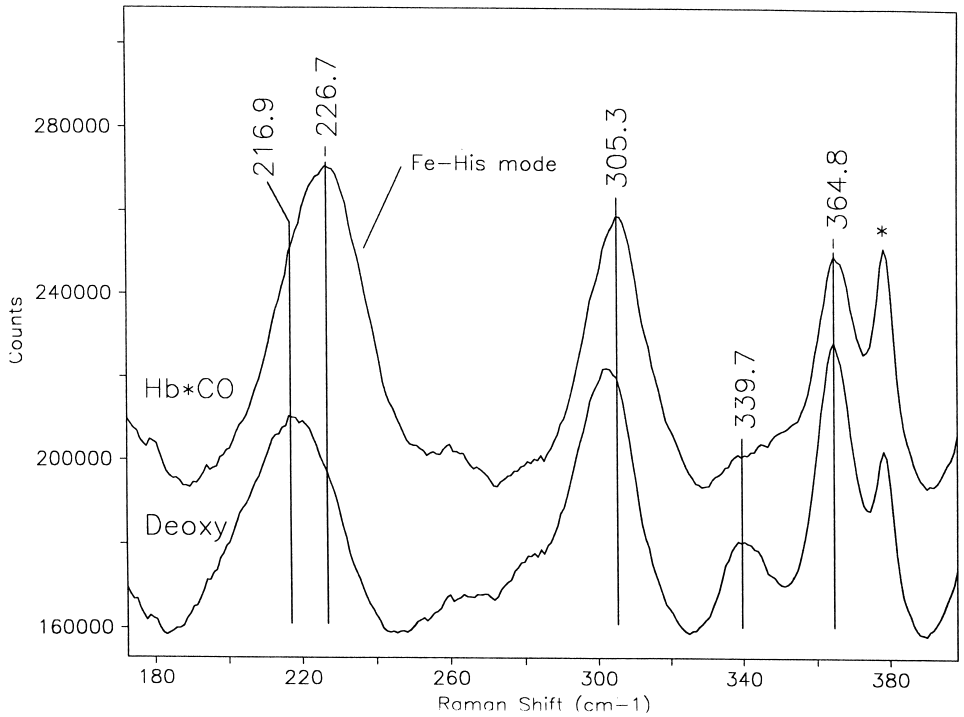

FIGURE 5: Low-frequency region of the visible resonance Raman spectra of the deoxy form and the 10 ns photoproduct (derived from the CO derivative and designated as Hb*CO in the figure) form of the double mutant recombinant hemoglobin at pH 7.0 (50 mM phosphate). The band labeled with asterisk is from the sapphire window of the sample cell.

displays a Y9a band at ~1174 cm^{-1} that shows little change upon the CO − deoxy transition.

rHb: Photoproduct versus Deoxy Visible Resonance Raman Spectra

Figure 5 shows the low-frequency region of the visible resonance Raman spectra of the equilibrium deoxy rHb and rHb*CO, the 10 ns photoproduct derived from the CO derivative of rHb under the same high phosphate solution conditions used in the UV Raman measurements. In contrast to the UV resonance Raman spectrum, which probes the aromatic amino acids, the visible resonance Raman spectrum probes the heme-related degrees of freedom. The visible resonance Raman spectra in the figure are in both instances probing a five-coordinate ferrous high-spin heme, but with different surrounding protein conformations. In the deoxy case, the surrounding protein is associated with the equilibrium deoxy tertiary structure; whereas, in the 10 ns photoproduct, the heme is being influenced by the still unrelaxed tertiary structure of the initial CO-bound derivative (Scott & Friedman, 1984; Friedman, 1994). The low-frequency band that occurs between 200 and 230 cm^{-1} in the spectra of five-coordinate ferrous hemes in which the fifth ligand is a histidine has been convincingly assigned to the iron-proximal histidine stretching mode (Argade et al., 1984; Kitagawa, 1988). The frequencies for this mode seen in Figure 5 for rHb are similar to what is observed for HbA under similar solution and excitation conditions (Friedman 1984, 1994; Rousseau & Friedman, 1988).

Both the change in the frequency (217 → 227 cm^{-1}) of the iron-proximal histidine stretching mode of rHb and the changes in the propionate sensitive modes between 340 and 370 cm^{-1} are characteristic of the tertiary and quaternary changes that occur upon going from the deoxy T state to the photoproduct of what is typically assumed to be a liganded R state. The 227 cm^{-1} frequency reflects a 3 cm^{-1} reduction from the anticipated 230 cm^{-1} value reported for the COHbA photoproduct (Friedman et al., 1983; Jayaraman et al., 1995). The reduction is readily attributed to the high phosphate concentration. The same effect is observed for COHbA (spectra not shown) when a slight excess of IHP (Scott et al., 1983, 1985; Scott & Friedman, 1984) or a large excess of phosphate (unpublished results) is added to the solution at pH values near 7.0 or lower. The frequency of the deoxy form of the rHb is slightly higher than what is observed for HbA but is still within the range of T state species (Kitagawa, 1988). This increased frequency is likely indicative of a destabilization of the deoxy T state for the double mutant, a conclusion consistent with the functional studies reported earlier (Kim et al., 1994).

Quaternary Structure Assignments

The changes in the visible resonance Raman spectra in going from the deoxy to the photoproduct forms of the rHb are consistent with what has traditionally been attributed to the T to R transition. The deoxy spectrum contains a frequency for the iron-proximal histidine stretching mode that is unmistakably characteristic of the T state, reflecting substantial proximal strain (compared to the R state). The corresponding frequency observed for the photoproduct is typical of R state photoproducts in the presence of allosteric effectors such as IHP or high concentrations of phosphate. It has usually been assumed that the CO-bound form of HbA and most high-affinity mutant forms of HbA are in the R quaternary state. An exception is COHb Ypsilanti (Asp β99 → Tyr) which, at least in the crystal, adopts a different quaternary state designated as Y (Smith et al., 1991). The Y state closely resembles the R2 state which has been observed for ligand bound derivatives crystallized from a low salt solution (Silva et al., 1992). The R2 structure has

also been observed for the cyanomet derivative of HbA in crystals grown under near-physiological conditions (Smith and Simmons, 1994). It is not as yet possible to establish whether the solution phase forms of COHb are in the R or R2 state. The visible resonance Raman spectrum of the photoproduct of COHb Ypsilanti (Friedman, unpublished results) is very similar to that obtained from COHbA, which further indicates the difficulty in spectroscopically distinguishing the two states. The solution conditions employed in the present study (high ionic strength) are thought to favor the R and not the R2 state. Given these solution conditions, but still recognizing the uncertainty in the quaternary assignment, we will assume for the purposes of the following discussion that the CO derivatives of both HbA and rHb are in the R state. In both the R and R2 structures, the α42−β99 hydrogen bond is lost so the germane issue is the determination of the nature of the T state hydrogen bond associated with this pair of residues. The exact identity of the ligand bound species is not crucial to the following analysis. The high concentrations of protein employed in these measurements also ensures against a significant contribution from dimers.

Origin of Tyrosine-Related UV Raman Differences

The presence of all the tryptophan markers in the CO − deoxy rHb UV Raman difference spectrum for the R − T transition coupled with the ligand-induced changes observed in the visible resonance Raman spectra makes a convincing case that rHb is undergoing the quaternary changes expected from the NMR and functional studies (Kim et al., 1994). The distinct diminution in the rHb UV difference spectrum of the tyrosine features associated with the Y9a, Y8a, and Y8b bands that are so prominent in the corresponding HbA UV Raman difference spectrum is most easily explained by the loss of Tyr α42.

The result presented above validates Rodgers et al. (1992) assumption that Y8a and Y8b frequency and intensity changes observed in HbA arise primarily from Tyr α42. Given the solid correlation (Rodgers et al., 1992; Hildebrandt et al., 1988) between changes in the intensity and frequency of these Raman bands and the nature of the hydrogen bonding pattern, it can be concluded that Tyr α42 must indeed be a proton acceptor in the deoxy T state.

A structural implication of Tyr α42 being a proton acceptor in the deoxy T state is that the carboxyl of Asp β99, the T state hydrogen bonding partner of Tyr α42, must remain protonated at neutral pH, as asserted by Spiro and co-workers. Spiro and co-workers (Rodgers et al., 1992) presented a series of plausible arguments that explain how the p*K*a of the T state Asp β99 carboxyl could be sufficiently elevated to account for the reversal of the anticipated H-bonding pattern. They show that the existing T state crystallographic data can accommodate a conformation in which a protonated Asp β99 forms the hydrogen bond to Tyr α42. They point out that aside from Tyr α42, Asp β99 is surrounded by hydrophobic groups in the T state structure and that the solvent accessible surface area is negligible as measured by the Lee and Richards (1971) rolling sphere method. Although there are four water molecules in the vicinity of Asp β99 (within 6 Å) seen in the crystal structure, they are all localized away from Asp β99 and appear hydrogen bonded to other residues. They conclude that these indications of a low dielectric constant could account for the increased p*K*a. A comparable assessment of the R state reveals an increase of 13% in the solvent accessible volume of the side chain. They also cite Karplus and co-workers (Gao et al., 1989) who find an additional two waters in the vicinity of Asp β99 side chain in the R state energy-minimized structure.

The concept of a high p*K*a for a protein carboxyl is not without precedent. Roa and Acharya (1992) presented evidence that the carboxyl group of Glu β43 in HbA has a high p*K*a in the deoxy T state that is attributed to the increased hydrophobicity of the T state $\alpha_1\beta_2$ interface.

R − T Changes in the Penultimate Tyrosines on the Basis of the UV Raman Spectra. Although the UV Raman difference spectrum for rHb shows fewer tyrosine related features compared to HbA, there does exist one obvious feature which indicates that Y8a increases in intensity upon deligation. As pointed out by Rodgers et al. (1992), Tyr α42 and the penultimate tyrosines are the only tyrosines that exhibit a quaternary state dependent change that might be reflected in the UV Raman spectrum. Since Tyr α42 is absent in rHb, the penultimate tyrosines are implicated as the source of the intensity change observed for Y8a in the rHb spectrum.

In going from the T to the R structure, the phenol side chains of the penultimate tyrosines remain within the H−F pockets but become more disordered (Shannon, 1983). In contrast, in the R2 state, the side chain of Tyr α140 is expelled from this pocket and becomes solvent exposed (Silva et al., 1992). Similarly, the Tyr β145 side is expelled from the H−F pocket in the Y structure of COHb Ypsilanti (Smith et al., 1991). The modest intensity changes in Y8a and the absence of other tyrosine-associated difference features in the rHb UV Raman difference spectrum is in conflict with a T to R2/Y transition since the escape of the phenol side chain from the H−F pocket would be expected to be accompanied by more significant changes in the tyrosine Raman bands. On the basis of the hydrogen bonding dependencies of this Raman band observed in a series of model systems (Rodgers et al., 1992; Austin et al., 1993), it can be concluded that the decrease in intensity indicates a decrease in hydrogen bond strength in going from T to R and that the tyrosine is the proton donor. The obvious source for this H-bonding change is an introduction of disorder in the hydrogen bonding pattern between the side chain carbonyl of the FG5 valines and the phenolic protons from the penultimate tyrosines (αHC2 and βHC2).

Contribution of Penultimate Tyrosines to Cooperativity and Reactivity. If, as the above analysis indicates, the hydrogen bond strength between the penultimate tyrosines and the FG5 valines is a function of quaternary state of the hemoglobin, then this has implications for the communication pathway between the conformational determinants of the quaternary state (e.g., the $\alpha_1\beta_2$ interface) and those that determine the proximal strain at the heme. The role of intra- and intersubunit contacts in the allosteric ligand binding function of HbA has been emphasized by the sterochemical model proposed by Perutz on the basis of crystallographic studies (Perutz et al., 1987; Perutz, 1989); however, the functional role of tyrosines at αHC2 and βHC2 has been somewhat controversial (*vide infra*).

The side chains of penultimate Tyr residues at αHC2 and βHC2 occupy the pockets made by the F and H helices in

the deoxy T state structure. The phenolic hydroxyl is hydrogen bonded to the carbonyl group of Val at FG5. In the T state, both the tyrosine and the entire C-terminus and its salt-bridged or hydrogen-bonded partners are highly ordered. Early crystallographic studies (Baldwin & Chothia, 1979) suggested that in the R form, the phenol side chains of the HC2 tyrosines are neither hydrogen bonded to the valines of the FG corner nor still in the F−H pocket. Without the H bond linkage, the tyrosine and the rest of the C-terminus become mobile and disordered in the electron density maps of oxyHb. This hydrogen bond has been considered to play an important role in maintaining the low-oxygen-affinity state (T state) in deoxy HbA.

A more recent high-resolution crystallographic study shows that these tyrosines do in fact remain within the F−H pocket, based on the electron density maps of oxyHb (Shaanan, 1983); however, the tyrosines do appear more disordered, suggestive of a weakening of the hydrogen bond to the FG corner valines as indicated from the present study. Two important questions remaining: (1) Are the hydrogen bonds between the HC2 tyrosines and the valines at the FG5 position needed to stabilize the T structure? (2) Does the strength of that hydrogen bond play a role in regulating reactivity at the heme?

The hydrogen bond per se does not appear to be a requirement for the formation of a stable T state structure. Instead, there is evidence (Ishimori et al., 1992) that it is the presence of the aromatic side chain in the F−H pocket that is required for T state stability. This point is made from the observations (Ishimori et al., 1992) of naturally occurring mutants of HbA such as Hb Osler (Tyr β145 → Asp), Nancy (Tyr β145 → Asp), rHb (Tyr β145 → Phe), and Hb McKees Rocks (Tyr β145 → terminated). In Hb Osler and McKees Rocks, there is essentially no cooperative ligand binding and the oxygen affinity is very high. X-ray crystallographic studies on Hb Nancy (Arnone et al., 1976) indicate that the carboxyl-terminal tetrapeptide is severely disordered in the deoxy form, and as a result the T state interactions of His β146(HC3) do not occur. In contrast the recombinant rHb (Tyr β145 → Phe) does not exhibit drastic changes in functional and structural parameters. rHb (Tyr β145 → Phe) binds oxygen cooperatively, and the oxygen affinity is only moderately increased. The NMR spectrum reveals that the deoxy form of this mutant does adopt the T state. The authors (Ishimori et al., 1992) conclude that in the natural mutants the substitutions for Tyr β145 are sufficiently extreme that the β145 residue side chains are no longer stable within the H−F pocket but that the side chain in Tyr β145 → Phe mutation can be accommodated within the H−F pocket. Furthermore, this conclusion indicates that the presence of the phenyl ring within the H−F pocket is sufficient to stabilize the T state interactions in the deoxy form of the Hb and that the hydrogen bond between the penultimate tyrosine and the valine at FG5 is not an absolute necessity, but only a modulating influence.

Our observation indicates a strengthening of the H−F hydrogen bond (Tyr HC2 and Val FG5) upon deoxygenation under conditions where it can be reasonably assumed that the phenol ring of the tyrosine remains within the H−F pocket. The remaining question is whether modulation of this hydrogen bond can act as a conduit for protein modulation of heme reactivity. Since these tyrosines couple the $\alpha_1\beta_2$ interface with the F helix through the valine at FG5, it is reasonable to think that this H-bond may be an important link between the quaternary structure and the local tertiary structure at the heme. This hypothesis is supported by the result from Ishimori et al. (1992) where the βHC2 Tyr → Phe substitution results in a cooperative protein, but with only moderately increased oxygen affinity. The visible resonance Raman spectrum of the deoxy form of this mutant reveals an iron-proximal histidine stretching frequency that is several cm^{-1} higher than for HbA. Such an increase is indicative of a reduction in proximal strain. This reduction in proximal strain is occurring despite the fact the deoxy form of this mutant Hb remains in the T structure (*vide supra*). Thus, the retention of the phenyl ring within the H−F pocket stabilizes the T state interactions, but the loss of the H−F hydrogen bond allows for a partial relaxation of proximal strain of the kind that typically occurs upon a switch to the R structure.

The hydrogen bond between the penultimate tyrosine and Val FG5 may provide a communication pathway between the $\alpha_1\beta_2$ interface and the heme via the F helix. In going from the T to the R state, the F helix shifts or slides away from the EF corner toward the FG corner. This shift results in a less strained proximal histidine orientation with respect to the heme [see, for example, Perutz (1989)]. A strong hydrogen bond between the tyrosine and the valine at the FG corner could favor a shift of the F helix toward the EF corner. A shift of the F helix toward the EF corner should result in increased proximal strain as seen in the T state. In the α subunits this proximal strain is manifest in an increase in the tilt of the proximal imidazole (with respect to an axis normal to the heme). A reduction in the H−F hydrogen bond strength would then result in a shift of the F helix toward the FG corner and reduce proximal strain. A possible counterpoint to the H−F effect is the binding of effectors to the DPG binding site. It is likely that effector binding to the DPG binding site favors a shift of the F helix toward the EF corner (possibly through Lys β82) as evidenced by the reduction in the frequency of the iron-proximal histidine stretching frequency upon addition of IHP to COHbA (Scott et al., 1983, 1985).

The idea that modulation of the H−F hydrogen bond can influence the heme via the above F helix shifting mechanism is supported by recent results (to be published) on a new cross-bridged HbA derivative, Bis Mal PEG2000. In this cooperative derivative of HbA, an intramolecular cross-bridge derived from bismaleido phenyl polyethylene glycol 2000 is inserted, resulting in bissuccinimydol phenyl polyethylene glycol being linked to the two Cys β93 residues (Acharya et al., 1996). The β93 residue is very close to the region of the penultimate tyrosine of the β subunit and, based on preliminary molecular modeling studies, the covalently linked moieties are likely to restrict motion of residues in the H−F pocket. If the Tyr β145 side chain is restricted in its motion and hence the degree of disorder reduced, a concomitant strengthening of the tyrosine to FG 5 valine hydrogen bond is anticipated. The UV resonance Raman shows changes in the CO-bound derivative of Bis Mal PEG2000−HbA that are consistent with a strengthening of the hydrogen bonding between the penultimate tyrosine and the valine at the FG corner (the CO − deoxy difference spectrum still shows the Tyr α42 associated changes). At the same time, the time-resolved visible resonance Raman of the photoproduct at 10 ns of the CO derivative shows a large decrease in the

frequency of the Fe−His stretching frequency, which is indicative of increased proximal strain within the R state. Similarly, there is a sizable decrease in the geminate yield of this CO derivative relative to COHbA, which is also consistent with increased proximal strain within the R state (Friedman et al., 1985). Together all of these results suggest that enhancement of the penultimate Tyr hydrogen bonding (possibly through a reduction in the mobility of the tyrosine side chain) results in enhanced proximal strain at the heme.

CONCLUSIONS

The results obtained in this study directly support the claim (Rodgers et al., 1992) that the T state hydrogen bond between Tyr α42 and Asp β99 has the tyrosine as the proton acceptor, which implies a relatively hydrophobic local environment for the carboxyl group of Asp β99. The absence of contributions from this pair of residues to the R − T difference spectrum of the double mutant allows for a clear observation of how other tyrosines participate in the quaternary switch. The results obtained are consistent with a T state strengthening of the hydrogen bond between the penultimate tyrosines and their hydrogen bonding partners at the FG corner. The current results indicate that this double mutant is of significant potential value in probing the functionally relevant status of the pocket derived from the overlap of the H and F helices (by monitoring the hydrogen bond strength of the penultimate tyrosine with the valine at position FG5) as a function of additional modifications and added allosteric effectors. By monitoring both the status of the H−F pocket and the Raman signal from the heme as a function of both time and systematic perturbations, it should be possible to test the proposed communication pathway implied by the present results.

REFERENCES

Abraham, D. J., Peascoe, R. A., Randad, R. S., & Panikker, J. (1992) *J. Mol. Biol. 227* (2), 480−450.

Acharya, A. S., Malavalli, A., Smith, P. K., & Manjula, B. N. (1996) *Artif. Cells, Blood Substitutes, Immobilization Biotechnol. 24*, 296A.

Ackers, G. K., Doyle, M. L., Myers, D., & Daugherty, M. A. (1992) *Science 255*, 54−63.

Antonini, E., & Brunori, M. (1971) *Hemoglobin and Myoglobin in Their Reactions with Ligands*, North-Holland Publishing, Amsterdam.

Argade, P. V., Sassaroli, M., Rousseau, D. L., Inubushi, T., Ikeda-Saito, M., & Lapidot, A. (1984) *J. Am. Chem. Soc. 106*, 6593−6596.

Arnone, A., Gacon, G., & Wajcman, H. (1976) *J. Biol. Chem. 251*, 5875−5884.

Arnone, A., Rogers, P., Blough, N. V., McGourty, J. L., Hoffman, B. M. (1986) *J. Mol. Biol. 188*, 693−706.

Asher, S. (1993) *Anal. Chem. 65*, 2.

Austin, J. C., Jordan, T., & Spiro, T. G. (1993) *Biomolecular Spectroscopy*, Part A, p 55, John Wiley & Sons, New York.

Baldwin, J. M., & Chothia, C. (1979) *J. Mol. Biol. 129*, 175.

Bonaventura, J., Bonaventura, C., Brunori, M., Gianadina, B., Antonini, E., Bossa, F., & Wyman, J. (1972) *Proc. Natl. Acad. Sci. U.S.A., 69*, 2174−2178.

Bucci, E., Fronticelli, C., Nicklas, J., & Charache, S. (1979) *J. Biol. Chem. 254*, 10811−10819.

Bucci, E., Fronticelli, C., Gryczynski, Z., Razynski, A., & Collins, J. H. (1993) *Biochemistry 32*, 3519.

Charache, S., Brimhall, B., & Jones, R. T. (1975) *Johns Hopkins Med. J. 136*, 132−136.

Dickerson, R. E., & Geis, I. (1983) *Hemoglobin Structure, Function, Evolution, and Pathology*, Benjamin/Cummings, Menlo Park, CA.

Fermi, G., Perutz, M. F., Shaanan, B., & Fourme, R. (1984), *175*, 159.

Friedman, J. M. (1985) *Science 228*, 1273−1280.

Friedman, J. M. (1994) *Methods Enzymol. 232*, 205−231.

Friedman, J. M., Rousseau, D. L., Ondrias, M. R., & Stepnoski, R. A. (1982) *Science 218*, 1244−1246.

Friedman, J. M., Scott, T. W., & Stepnoski, R. A. (1983) *J. Biol. Chem. 258*, 10564−10572.

Friedman, J. M., Scott, T. W., Fisanick, G. J., Simon, S. R., Findsen, E. W., Ondrias, M. R., MacDonald, V. W. (1985) *Science 229*, 187−190.

Fung, L. W.-M., & Ho, C. (1975) *Biochemistry 14*, 2526−2535.

Fung, L. W.-M., Minton, A. P., & Ho, C. (1976) *Proc. Natl. Acad. Sci. U.S.A. 73*, 1581−1585.

Fung, L. W.-M., Minton, A. P., Lindstrom, T. R., Pisciatta, A. V., & Ho, C. (1977) *Biochemistry 16*, 1452−1462.

Gao, J., Kuczera, K., Tidor, B., & Karplus, M. (1989) *Science 244*, 1069.

Gellin, B. R., Lee, A. W.-M., & Karplus, M. (1983) *J. Mol. Biol. 171*, 489−559.

Hashimoto, M., Ishimori, K., Imai, K., Miyazaki, G., Morimoto, H., Wada, Y., & Morishima, I. (1993) *Biochemistry 32*, 13688−13695.

Hayashi, A., & Stamatoyannopoulos, G. (1972) *Nature New Biol. 235*, 70−72.

Hildebrandt, P. G., Copeland, R. A., Spiro, T. G., Otlewski, J., Laskowski, M., & Prendergast, F. G. (1988) *Biochemistry 27*, 5424−5426.

Hirsch, R. E., Lin, M. J., Vidugirus, G. V. A., Huang, S., Friedman, J. M., & Nagel, R. L. (1996) *J. Biol. Chem. 271*, 372−375.

Ho, C. (1992) *Adv. Protein Chem. 43*, 153−312.

Imai, K., Fushitani, K., Miyazak, G., Ishimori, K., Kitagawa, T., Wada, Y., Morimoto, H., Morishima, I., Shih, D., & Tame, J. (1991) *J. Mol. Biol. 218*, 769−778.

Ishimori, K., Imai, K., Miyazaki, G., Kitagawa, T., Wada, Y., Morimoto, H., & Morishima, I. (1992) *Biochemistry 31*, 3256−3264.

Jayaraman, V., Rodgers, K. R., Mukerji, I., & Spiro, T. G. (1993) *Biochemistry 32*, 4547−4551.

Jayaraman, V., Rodgers, K. R., Mukerji, I., & Spiro, T. G. (1995) *Science 269*, 1843.

Jones, R. T., Osgood, E. E., Brimhall, B., & Koler, R. D. (1967) *J. Clin. Invest. 46*, 1840−1847.

Kim, H.-W., Shen, T.-J., Sun, D., Ho, N. T., Madrid, M., Tam, M. F., Zou, M. F., Cottam, P. F., & Ho, C. (1994) *Proc. Natl. Acad. Sci. U.S.A. 91*, 11547−11551.

Kim, H.-W., Shen, T.-J., Sun, D. P., Ho, N. T., Madrid, M., & Ho, C. (1995) *J. Mol. Biol. 248*, 867−882.

Kim, H.-W., Shen, T.-J., Sun, D. P., Ho, N. T., Zou, M., Tam, M., & Ho, C. (1996) *Biochemistry 35*, 6620−6627.

Kitagawa, T. (1988) *in Biological Application of Raman Spectroscopy* (Spiro, T. G., Ed.) Vol. 3, pp 97−131, Wiley & Sons, New York.

Kitagawa, T. (1992) *Prog. Biophys. Mol. Biol. 58*, 1−18.

Lee, B., & Richards, F. M. (1971) *55*, 379.

LiCata, V. J., Dalessio, P. M., & Ackers, G. K (1993) *Proteins: Structure, Funct., Genet. 17*, 279−296.

Liddington, R. (1994) *Methods Enzymol. 232C*, 15−26.

Nagai, M., Kaminaka, S., Ohba, Y., Nagai, Y., Mizutani, Y., & Kitagawa, T. (1995) *J. Biol. Chem. 270*, 1636−1642.

Perutz, M. F. (1989) *Q. Rev. Biophys. 22*, 139−236.

Perutz, M. F., Fermi, G., Luisi, B., Shaanan, B., & Liddington, R. C. (1987) *Acc. Chem. Res. 20*, 309.

Rao, M. J., & Acharya. A. S.(1992) *Biochemistry 31*, 7231−7236.

Reed, C. S., Hampson, R., Gordon, S. Jones, R. T., Novy, M. J., Brimhall, B., Weatherall, D. J., Clegg, J. B., Callender, S. T., Well, R. M. G., Henhns, E. R., Perutz, M. F., Viggiano, G., & Ho, C. (1977) *Br. J. Haematol.* 35, 177−191.

Rodgers, K. R., Su. C., Subramaniam, S., & Spiro, T. G. (1992) *J. Am. Chem. Soc. 114*, 3697−3709.

Rousseau, D. L., & Friedman, J. M. (1988) in *Biological Applications of Raman Spectroscopy* (Spiro, T. G., Ed.) Vol. 3, p 133, Wiley & Sons, New York.

Rucknagel, D. L., Glynn, K. P., & Smith, J. R. (1967) *Clin. Res. 15*, 270.

Schroeder, W. A., & Huisman, T. H. J. (1980) *The Chromatography of Hemoglobin*, p 61, Marcel Dekker, Inc., New York.

Scott, T. W., & Friedman, J. M. (1984) *J. Am. Chem. Soc. 106*, 5677−5687.

Scott, T. W., Friedman, J. M., Ikeda-Saito, M., & Yonetani, T. (1983) *FEBS Lett. 158*, 69−72.

Scott, T. W., Friedman, J. M., & Macdonald, V. W. (1985) *J. Am. Chem. Soc. 107*, 3702−3705.

Shaanan, B. (1983) *J. Mol. Biol. 171*, 31−33.

Shen, T. J., Ho, N. T., Simplaceanu, V., Zou, M., Green, B. N., Tam, M. F., & Ho, C. (1993) *Proc. Natl. Acad. Sci. U.S.A. 90*, 8108−8112.

Silva, M. M., Rogers, P. H., & Arnone, A. (1992) *J. Biol. Chem. 267*, 17248−17256.

Smith, F. R., Simmons, K. C. (1994) *Proteins 18*, 295−300.

Srinivasan, R., Rose, G. D. (1994) *Proc. Natl. Acad. Sci. U.S.A. 91*, 11113−11117.

Togi, A., Ishimori, K., Unno, M., Konno T., Morishima, I., Miyazaki, G., & Imai, K. (1993) *Biochemistry 32*, 10165−10169.

Viggiano, G., & Ho, C. (1979) *Proc. Natl. Acad. Sci. U.S.A. 26*, 3673−3677.

Viggiano, G., Wiechelman, K. J., Chervenicko, P. A., & Ho, C. (1978) *Biochemistry 17*, 795−799.

BI970018V